Performance of Joint Source-Channel Coding Based on Protograph LDPC Codes over Rayleigh Fading Channels

Huihui Wu, Lin Wang, *Senior Member, IEEE*, Shaohua Hong, and Jiguang He

***Abstract*—This letter presents a joint protograph extrinsic information transfer (PEXIT) analysis for joint source and channel coding (JSCC) with double protograph-based low-density parity-check (DP_LDPC) codes over single-input multiple-output (SIMO) Rayleigh fading channels. The impacts of source statistics and receive antenna diversity on convergence performance for the JSCC are investigated, and we find that source sparsity plays a more vital role than diversity orders in improving both convergence and error performances under fading environments.**

***Index Terms*—Joint source-channel coding (JSCC), joint PEXIT analysis, source statistics, receive antenna diversity, Rayleigh fading channels.**

I. Introduction

In the presence of different approaches to joint source-channel coding (JSCC), an innovative structure that employs low-density parity-check (LDPC) codes as both source and channel codes [1], [2], referred to as double LDPC (D_LDPC) codes, has been illustrated to outperform tandem coding structures. However, the LDPC codes utilized in [1] and [2] are regular and irregular, which suffer from high error-floor and computational complexity. Therefore, protograph-based LDPC codes [3] have been introduced into D_LDPC systems (DP_LDPC in the following) by [4], where the error performance can be improved significantly. Moreover, the DP_LDPC codes have also been employed to transmit images over additive white Gaussian noise (AWGN) channels [5], and simulation results demonstrated that a reduction of channel signal-to-noise ratio (SNR) can be obtained while a large peak SNR (PSNR) gain can also be achieved.

Despite the fact that DP_LDPC codes perform well over AWGN channel, it may not work well in a fading environment. Although protograph extrinsic information transfer (PEXIT) algorithms [6] have been further tailored to predict the decoding thresholds of protograph-based codes over single-input multiple-output (SIMO) fading channels [7], to the best of our knowledge, little is known on the analytical performance for DP_LDPC codes considering both source statistics and multiple receive antennas under fading conditions.

In this letter, we present a joint PEXIT analysis for JSCC using DP_LDPC codes over Rayleigh fading channels, and the proposed algorithm concentrates on receive antenna diversity and source statistics. We then analyze the decoding thresholds of DP_LDPC codes to predict the error performance in the waterfall region. Simulation results show that decoding thresholds and error performance are more sensitive to source sparsity than diversity orders. Therefore, sparse representation of sources should be more concerned to obtain good decoding convergence behavior for JSCC systems in fading situations.

Manuscript received January 17, 2014. The associate editor coordinating the review of this letter and approving it for publication was S. Yousefi.

This work was supported by the National Natural Science Foundation of China (No. 61271241 and No. 61102134), and the European Union-FP7 (CoNHealth, Grant No. 294923).

H. Wu, L. Wang, and S. Hong are with the Department of Communication Engineering, Xiamen University, Xiamen, 361005, P. R. China. L. Wang is the corresponding author (e-mail: wanglin@xmu.edu.cn).

J. He is with the Department of Electronic Engineering, City University of Hong Kong, Kowloon, Hong Kong.

Digital Object Identifier 10.1109/LCOMM.2014.022714.140112

II. System Model

Considering that Markov source structures may be limited in many applications scenarios, such as speech recognition, image segmentation, etc [8]. This paper focuses on the more general case of hidden Markov model (HMM), where the state of the model is related to the output probabilistically as opposed to deterministically. We consider an HMM with $S = 2$ states can be defined by the vector$[a_{00}, a_{11}, b_{00}, b_{11}]$, where $a_{ij} = P_t(S_j|S_i)$denotes the probability of transition from state S_i to $S_j, 0 \leq i, j \leq S-1$, and $b_{ie} = P_o(e|S_i)$ represents the probability of getting the binary output e in state S_i. Moreover, P_1 is defined as the stationary probability of the symbols 1.

Let $\mathbf{w} = w_1 w_2 \cdots$ be the source sequence that takes values $w_k \in \{0, 1\}$ and is generated by an HMM. Then the source sequence is compressed by an unpunctured protograph LDPC code into binary sequence $\mathbf{b}$, followed by another protograph LDPC code to generate channel codeword $\mathbf{c}$. Subsequently, the codeword is passed to a binary-phase-shift-keying (BPSK) modulator, and the output of which is denoted by $\mathbf{x}$. The modulated signal is further sent to the SIMO Rayleigh fading channel with one transmit antenna and N_r receive antennas.

Let $\mathbf{h}$ be the channel vector of size $N_r \times 1$, whose entries are independent, complex, zero-mean, Gaussian variables with independent real and imaginary components having the same variance $1/2$. We define $\mathbf{n}$ as a $N_r \times 1$ complex Gaussian background noise with mean zero and covariance matrix $\sigma_n^2 \mathbf{I}$, where $\mathbf{I}$ represents the $N_r \times N_r$ identity matrix. Then, the receiver sees $N_r \times 1$ signal vectors

$$\mathbf{y} = \mathbf{h}x + \mathbf{n} \tag{1}$$

Assuming that $\mathbf{h}$ is perfectly known to the receiver, and it changes for every symbol $\mathbf{x}$ to satisfy ergodicity, and then the capacity of an ergodic SIMO channel is further given by [9]

$$H(\mathbf{w})R_c < C = E\left(\log_2 \det\left(\mathbf{I} + \frac{E_s}{N_0}\mathbf{h}\mathbf{h}^\dagger\right)\right),$$
$$H(\mathbf{w}) \leq R_s \tag{2}$$

where $H(\mathbf{w})$ is the source entropy, E_s denotes the average energy per transmitted symbol, and $\mathbf{h}^\dagger$ is the complex-conjugate

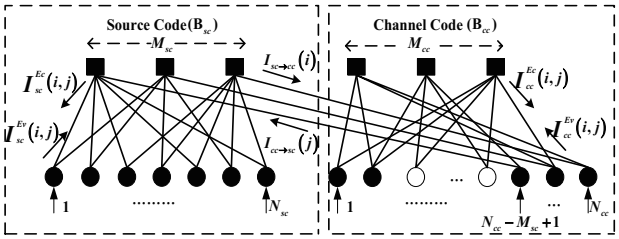

Fig. 1. Tanner graph representing the JSC decoder. The variable nodes connected to the channel are depicted with dark circles while check nodes are those dark squares, and blank circles denote the punctured variable nodes.

transpose of $\mathbf{h}$. R_s and R_c represent source code and channel code rates, respectively.

At the receiving terminal, the maximal-ratio combining (MRC) method is utilized to combine corrupted signals, and the output of which can be computed as $z_j = \sum_{r=1}^{N_r} h_j^*[r]y_j[r]$, where j indicates the coded bit number and $r(r = 1 \cdots N_r)$ marks the receive antenna number, *denotes the complex conjugate. The joint source and channel (JSC) decoder [4] is further implemented to decode the combined signals. Moreover, the definition of E_b/N_0 (E_b is the average energy per information bit) is expressed as

$$\frac{E_b}{N_0} = \frac{(N_r/R_c)E_s}{N_0} \tag{3}$$

In this letter, we assume that E_s is normalized to be 1, and then combining it with $N_0 = 2\sigma_n^2$ gives

$$\sigma_n^2 = \frac{N_r}{2R_c(E_b/N_0)} \tag{4}$$

III. Joint PEXIT Algorithm for DP_LDPC Codes

A. Assumptions of joint PEXIT algorithm

We first assume that the all-zero codeword is transmitted. Moreover, if a fixed channel vector $\mathbf{h}_j$ is given for the jth coded bit, the associated initial channel log-likelihood ratio (LLR) with MRC method has been proved to follow a symmetric complex Gaussian distribution, and it can be expressed as [7]

$$L_{ch,j} = \ln\left(\frac{P_r\left(c_j = 0|z_j, \mathbf{h}_j\right)}{P_r\left(c_j = 1|z_j, \mathbf{h}_j\right)}\right) \sim CN\left(\frac{2}{\sigma_n^2}f_j, \frac{4}{\sigma_n^2}f_j\right). \tag{5}$$

where c_j denotes the jth codeword bit mapped onto the vector symbol $\mathbf{x}$, and

$$f_j = \sum_{r=1}^{N_r} |h_j[r]|^2. \tag{6}$$

is defined as channel factor. Thus, the joint PEXIT algorithm can be analyzed over SIMO fading channels with this property.

B. Joint PEXIT algorithm for DP_LDPC codes

Fig.1 shows the Tanner graph of the JSC decoder, where the mutual information (MI) flow is also illustrated. A protograph with N variable nodes and M check nodes can be denoted by a base matrix $\mathbf{B}$ of dimension $M \times N$. Accordingly, $\mathbf{B}_{cc}$ with dimension $M_{cc} \times N_{cc}$ and $\mathbf{B}_{sc}$ with size of $M_{sc} \times N_{sc}$ represent the base matrices of channel code and source code, respectively. Besides, an assumption is made that the last M_{sc} variable nodes in $\mathbf{B}_{cc}$ are connected to the check nodes in $\mathbf{B}_{sc}$, and each check node is connected to only a single variable node. The (i,j)th element of $\mathbf{B}_{cc}(\mathbf{B}_{sc})$, denoted by $b_{cc}^{i,j}(b_{sc}^{i,j})$,represents the number of edges connecting the variable node v_j to check node c_i. Moreover, seven types of MI are defined as follows (with subscripts sc and cc indicating the source code $\mathbf{B}_{sc}$ and channel code $\mathbf{B}_{cc}$, respectively):

1) $I_{sc(cc)}^{A_v}(i,j)$: the a prior MI between input LLR of v_j on each of the $b_{sc(cc)}^{i,j}$ edges and the associated codeword bit v_j.

2) $I_{sc(cc)}^{A_c}(i,j)$: the a prior MI between input LLR of c_i on each of the $b_{sc(cc)}^{i,j}$ edges and the associated codeword bit v_j.

3) $I_{sc(cc)}^{E_v}(i,j)$: the extrinsic MI between the LLR sent by v_j to c_i and the corresponding codeword bit v_j.

4) $I_{sc(cc)}^{E_c}(i,j)$: the extrinsic MI between the LLR sent by c_i to v_j and the corresponding codeword bit v_j.

5) $I_{cc\to sc}(j)$: the extrinsic MI between the LLR sent by v_j in $\mathbf{B}_{cc}$ to c_i in $\mathbf{B}_{sc}$ and the associated codeword bit, on each of the last m_{sc} edges connecting v_j in $\mathbf{B}_{cc}$ to c_i in $\mathbf{B}_{sc}$.

6) $I_{sc\to cc}(i)$: the extrinsic MI between the LLR sent by c_i in $\mathbf{B}_{sc}$ to v_j in $\mathbf{B}_{cc}$ and the associated codeword bit, on each of the edges connecting c_i in $\mathbf{B}_{sc}$ to v_j in $\mathbf{B}_{cc}$.

7) $I_{sc}^{APP}(j)$: the MI between a posteriori LLR evaluated by v_j in $\mathbf{B}_{sc}$ and the associated codeword bit w_j.

In addition, the punctured label P_j of a variable node v_j is defined to be 0 if v_j is punctured and 1 otherwise.

We denote with $J(\sigma_{ch})$ the MI between a codeword bit and its corresponding LLR value $L_{ch} \sim N(\sigma_{ch}^2/2, \sigma_{ch}^2)$, and it is given by [9]

$$J(\sigma_{ch}) = 1 - \int_{-\infty}^{\infty} \frac{e^{-(\xi-\sigma_{ch}^2/2)^2/2\sigma_{ch}^2}}{\sqrt{2\pi\sigma_{ch}^2}} \cdot \log_2(1+e^{-\xi})\mathrm{d}\xi \tag{7}$$

Then, the joint PEXIT algorithm for DP_LDPC codes over SIMO Rayleigh fading channels is described as follows:

1) Channel Decoder

· **Channel factors realization**

Suppose we are given a channel vector $\mathbf{h} = [h[1], \cdots h[N_r]]^T$ and the number of blocks of channel factors (denoted by K), a matrix $\mathbf{F} = (f_{k,j}) = \left(\sum_{r=1}^{N_r} |h_{k,j}[r]|^2\right)$ of dimension $K \times N_{cc}$ is generated to represent the K blocks of channel factors, with each row in $\mathbf{F}$ indicating a group of channel factors for the N_{cc} variable nodes of channel codes.

· **Initialization**

Considering the punctured label P_j and the channel factor $f_{k,j}(j = 1, 2 \cdots N_{cc}$ and $k = 1, 2 \cdots K)$, the corresponding variance of initial LLR value $(\sigma_{ch,k,j}^2)$ can be given by [7]

$$\sigma_{ch,k,j}^2 = \frac{4P_j f_{k,j}}{\sigma_n^2} = \frac{8R_c P_j f_{k,j}}{N_r} 10^{((E_b/N_0)/10)} \tag{8}$$

where E_b/N_0 is in dB herein.

· **Variable nodes to check nodes update**

For $j = 1 \cdots N_{cc} - M_{sc}$ and $i = 1 \cdots M_{cc}$, if $b_{cc}^{i,j} \neq 0$,

$$I_{cc}^{E_v,k}(i,j) = J\left(\sqrt{\sum_{s\neq i} b_{cc}^{s,j}[J^{-1}(I_{cc}^{A_v}(s,j))]^2 + (b_{cc}^{i,j}-1)[J^{-1}(I_{cc}^{A_v}(i,j))]^2 + \sigma_{ch,k,j}^2}\right).$$

For $j = N_{cc}-M_{sc}+1 \cdots N_{cc}$ and $i = 1 \cdots M_{cc}$, if $b_{cc}^{i,j} \neq 0$,

$$I_{cc}^{E_v,k}(i,j) = J\left(\sqrt{\sum_{s\neq i} b_{cc}^{s,j}[J^{-1}(I_{cc}^{A_v}(s,j))]^2 + (b_{cc}^{i,j}-1)[J^{-1}(I_{cc}^{A_v}(i,j))]^2 + \sigma_{ch,k,j}^2 + [J^{-1}(I_{sc\to cc}(j-(N_{cc}-M_{sc})))]^2}\right).$$

If $b_{cc}^{i,j} = 0, I_{cc}^{E_v,k}(i,j) = 0$.

· For $j = 1 \cdots N_{cc}$ and $i = 1 \cdots M_{cc}$, we obtain the average MI of $I_{cc}^{E_v,k}(i,j)$ by

$$E[I_{cc}^{E_v,k}(i,j)] = \frac{1}{K}\sum_{k=1}^{K} I_{cc}^{E_v,k}(i,j) \tag{9}$$

and set $I_{cc}^{A_c}(i,j) = E[I_{cc}^{E_v,k}(i,j)]$.

· **Check nodes to variable nodes update**

For $j = 1 \cdots N_{cc}$ and $i = 1 \cdots M_{cc}$, if $b_{cc}^{i,j} \neq 0$,

$$I_{cc}^{E_c}(i,j) = 1 - J\left(\sqrt{(\sum_{s\neq j} b_{cc}^{i,s}[J^{-1}(1-I_{cc}^{A_c}(i,s))]^2) + (b_{cc}^{i,j}-1)[J^{-1}(1-I_{cc}^{A_c}(i,j))]^2}\right).$$

Set $I_{cc}^{A_v}(i,j) = I_{cc}^{E_c}(i,j)$; and if $b_{cc}^{i,j} = 0, I_{cc}^{E_c}(i,j) = 0$.

· **Variable nodes in $\mathbf{B}_{cc}$ to check nodes in $\mathbf{B}_{sc}$update**

For $j = N_{cc}-M_{sc}+1 \cdots N_{cc}$ and $i = 1 \cdots M_{cc}$, if $b_{cc}^{i,j} \neq 0$,

$$I_{cc\to sc,k}(j-(N_{cc}-M_{sc})) = J\left(\sqrt{(\sum_{i} b_{cc}^{i,j}[J^{-1}(I_{cc}^{A_v}(i,j))]^2) + \sigma_{ch,k,j}^2}\right).$$

Then the MI is further averaged by

$$I_{cc\to sc}(j-(N_{cc}-M_{sc})) = \frac{1}{K}\sum_{k=1}^{K} I_{cc\to sc,k}(j-(N_{cc}-M_{sc})). \tag{10}$$

2) Source Decoder

· **Initialization**

A "virtual" channel corresponding to the source with noise distribution identical to the source statistics can be modeled by a binary symmetric channel (BSC) with crossover probability denoted by P_1. The probability density function of the LLR output from the equivalent channel is expressed as $P_1\delta(\psi + L_{sc}) + (1-P_1)\delta(\psi - L_{sc})$, $L_{sc} = \ln((1-P_1)/P_1)$. Then we denote with $J_{BSC}(\cdot)$ a manipulation of the function $J(\cdot)$ to take source statistics P_1 into account, and it is given by [2]

$$J_{BSC}(\mu, P_1) = (1-P_1)I(V;\chi^{(1-P_1)}) + P_1 I(V;\chi^{P_1}). \tag{11}$$

where $\chi^{(1-P_1)} \sim N(\mu+L_{sc}, 2\mu)$, $\chi^{(P_1)} \sim N(\mu-L_{sc}, 2\mu)$; $I(V;\chi)$ is the MI between LLR value of v_j in $\mathbf{B}_{sc}$ and χ. μ represents the average LLR value obtained by variable node v_j in $\mathbf{B}_{sc}$.

· **Variable nodes to check nodes update**

For $j = 1 \cdots M_{sc}$ and $i = 1 \cdots N_{sc}$, if $b_{sc}^{i,j} \neq 0$,

$$I_{sc}^{E_v}(i,j) = J_{BSC}\left(\sum_{s\neq i} b_{sc}^{s,j}[J^{-1}(I_{sc}^{A_v}(s,j))]^2 + (b_{sc}^{i,j}-1)[J^{-1}(I_{sc}^{A_v}(i,j))]^2, P_1\right).$$

Set $I_{sc}^{A_c}(i,j) = I_{sc}^{E_v}(i,j)$; and if $b_{sc}^{i,j} = 0, I_{sc}^{E_v}(i,j) = 0$.

· **Check nodes to variable nodes update**

For $j = 1 \cdots N_{sc}$ and $i = 1 \cdots M_{sc}$, if $b_{sc}^{i,j} \neq 0$,

$$I_{sc}^{E_c}(i,j) = 1 - J\left(\sqrt{\sum_{s\neq j} b_{sc}^{i,s}[J^{-1}(1-I_{sc}^{A_c}(i,s))]^2 + (b_{sc}^{i,j}-1)[J^{-1}(1-I_{sc}^{A_c}(i,j))]^2 + [J^{-1}(1-I^{cc\to sc}(i))]^2}\right).$$

Set $I_{sc}^{A_v}(i,j) = I_{sc}^{E_c}(i,j)$; and if $b_{sc}^{i,j} = 0, I_{sc}^{E_c}(i,j) = 0$.

· **Check nodes in $\mathbf{B}_{sc}$ to variable nodes in $\mathbf{B}_{cc}$ update**

For $j = 1 \cdots N_{sc}$ and $i = 1 \cdots M_{sc}$, if $b_{sc}^{i,j} \neq 0$,

$$I_{sc\to cc}(i) = 1 - J\left(\sqrt{\sum_{j} b_{sc}^{i,j}[J^{-1}(1-I_{sc}^{A_c}(i,j))]^2}\right).$$

· **APP-LLR mutual information evaluation**

For $j = 1 \cdots N_{sc}$ and $i = 1 \cdots M_{sc}$, if $b_{sc}^{i,j} \neq 0$,

$$\mu(j) = \sum_{i} b_{sc}^{i,j}[J^{-1}(I_{sc}^{A_v}(i,j))]^2,$$

$$I_{sc}^{APP}(j) = J_{BSC}(\mu(j), P_1). \tag{12}$$

· **Iterate until** $I_{sc}^{APP}(j) = 1, \forall j$.

Note that each of the output extrinsic MI sent by variable node v_j in $\mathbf{B}_{cc}$ (i.e. $I_{cc}^{E_v,k}(i,j)$ and $I_{cc\to sc,k}(j)$) depends on both the initial channel LLR $\sigma_{ch,k,j}^2$ and the type of code used. Therefore, we need to compute the average values ((9) and (10)) based on the K blocks of channel factors. Moreover, K should be generated sufficiently large to simulate the ergodic fading channel that implemented by independent realizations of $\mathbf{h}$. In this letter, we set $K = 10^5$.

IV. Simulation Results and Discussion

In this paper, the rate 1/2 accumulate-repeat-by-3-accumulate (AR3A) code is employed as channel code and repeat-by-4-jagged-accumulate (R4JA) code with rate 1/4 [10] is utilized as source code, whose corresponding base matrices (denoted by $\mathbf{B}_{cc}^{AR3A}$ and $\mathbf{B}_{sc}^{R4JA}$, respectively) are given by

$$\mathbf{B}_{cc}^{AR3A} = \begin{bmatrix} 1 & 2 & 1 & 0 & 0 \\ 0 & 2 & 1 & 1 & 1 \\ 0 & 1 & 2 & 1 & 1 \end{bmatrix} \tag{13}$$

$$\mathbf{B}_{sc}^{R4JA} = \begin{bmatrix} 3 & 1 & 3 & 1 & 3 & 1 & 1 & 1 \\ 1 & 2 & 1 & 3 & 1 & 3 & 1 & 2 \end{bmatrix} \tag{14}$$

Note that the variable nodes associated with the second columns in (13) are punctured. Moreover, we terminate the simulation after 800 bit errors are detected at each E_b/N_0, and the JSC decoder performs a maximum of 100 BP iterations for each frame.

TABLE I
DECODING THRESHOLDS AND CAPACITY (E_b/N_0) CONSIDERING SOURCE STATISTICS AND DIVERSITY ORDERS OVER SIMO FADING CHANNEL.

HMM	P_1	Entropy $H(\mathbf{w})$	Capacity E_b/N_0(dB)		Decoding thresholds E_b/N_0(dB)					
			$N_r=1$	$N_r=4$	$N_r=1$	Gap Δ	$N_r=2$	$N_r=3$	$N_r=4$	Gap Δ
$[0.02, 0.02, 0.99, 0.01]$	0.01	0.08	-1.47	-1.51	-0.31	1.16	-0.86	-1.06	-1.14	0.37
$[0.03, 0.04, 0.98, 0.01]$	0.015	0.11	-1.43	-1.48	0.48	1.91	-0.12	-0.34	-0.46	1.02
$[0.02, 0.02, 0.98, 0.02]$	0.02	0.14	-1.38	-1.45	1.12	2.50	0.4	0.14	0.04	1.49
$[0.03, 0.03, 0.96, 0.01]$	0.025	0.17	-1.36	-1.44	1.48	2.84	0.75	0.47	0.38	1.82

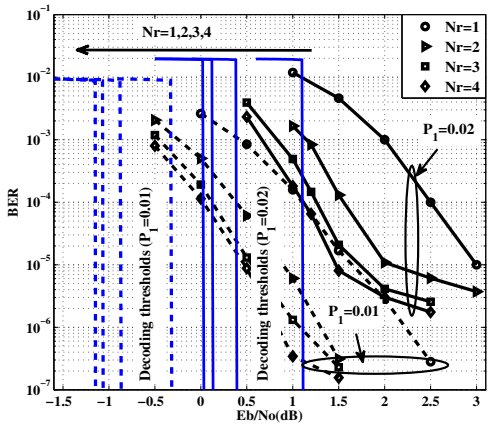

Fig. 2. Performance comparisons for source statistics $P_1 = 0.01, 0.02$ with diversity orders $N_r = 1, 2, 3, 4$ over Rayleigh fading channels.

In order to assess the system performance, we simulate the proposed joint PEXIT algorithm for sources generated by different HMMs, which result in different entropies. The frame length is fixed to 3200 bits.

The decoding thresholds and capacity at E_b/N_0 of DP_LDPC codes for different source statistics with diversity orders $N_r = 1, 2, 3, 4$ are illustrated in Table. I (For our simulation, each channel formed by one transmit-receive antenna pair is faded independently and hence the diversity order equals N_r). The results indicate that the decoding thresholds can be reduced either by making sources sparser (lower P_1 or source entropy) or employing more receive antennas (higher implementation complexity), and the reduction rate of decoding thresholds slows down as N_r is incremented while the rate accelerates with entropy decreases. Therefore, sparse representation of sources plays a more important role than diversity orders in lowering decoding thresholds over Rayleigh fading channels, and the lower decoding thresholds suggest better error performance in the low-SNR region. Moreover, the capacity gaps between channel capacity and decoding thresholds for $N_r = 1$ and 4 narrows as the source entropy goes down, i.e., the smallest gap (0.37 dB in the simulation) can be obtained for sparse sources with high diversity order.

Fig. 2 plots the bit error rate (BER) curves of DP_LDPC codes over SIMO Rayleigh fading channel for different source statistics. It can be noted that the sparser source achieves better error performance for all diversity orders under study. More specifically, the DP_LDPC scheme with one receive antenna for source statistics $P_1 = 0.01$ outperforms that with four receive antennas for source statistics $P_1 = 0.02$ in the low-SNR region. Besides this, exploiting more receive antennas simply makes no sense to lower the error floor if source statistics being ignored. Moreover, the sparser source contributes more to improving convergence performance than the diversity order, due to less reduction on decoding thresholds can be obtained by increasing receive antennas. Accordingly, source statistics (sparsity) should be considered principally in order to design the appropriate capacity-approaching LDPC codes for JSCC systems over Rayleigh fading channels.

V. CONCLUSION

In this letter, a joint PEXIT algorithm considering source statistics and multiple receive antennas for JSCC with protograph LDPC codes over Rayleigh fading channels has been developed. The decoding thresholds have also been analyzed by the presented joint PEXIT algorithm. Numerical results have revealed that source sparsity has a more important impact on decoding thresholds and BER performance than receive antenna diversity for JSCC systems in a fading situation.

REFERENCES

[1] M. Fresia, F. Perez-Cruz. and H. V. Poor, "Optimized concatenated LDPC codes for joint source-channel coding," in *Proc. 2009 Int. Symp. Information Theory,* pp. 2131–2135.
[2] M. Fresia, F. Perez-Cruz, H. V. Poor, and S. Verdu, "Joint source and channel coding," *IEEE Signal Process. Mag.,* vol. 27, no. 6, pp. 104–113, Nov. 2010.
[3] J.Thorpe, "Low-density parity-check (LDPC) codes constructed from protographs," *IPN Progress Report,* pp. 42–154, Aug. 2003.
[4] J. He, L. Wang, and P. Chen, "A joint source and channel coding scheme base on simple protograph structured codes," in *Proc. 2012 Int. Symp. Communications and Information Technologies,* pp. 65–69.
[5] L. Xu, H. Wu, J. He, and L. Wang, "Unequal error protection for radiography image transmission using protograph double LDPC codes," in *Proc. 2013 Int. Symp. Wireless Telecommunications,* pp. 1–5.
[6] G. Liva and M. Chiani, "Protograph LDPC codes design based on EXIT analysis," in *Proc. 2012 Global Telecommunications Conf.,* pp. 3250–3254.
[7] Y. Fang, P. Chen, L. Wang, F. C. M. Lau, and K.-K. Wong, "Performance analysis of protograph-based low-density parity-check codes with spatial diversity," *IET Commun.,* vol. 6, no. 17, pp. 2941–2948, Nov. 2012.
[8] L. Rabiner, "A tutorial on hidden Markov models and selected applications in speech recognition," *Proc. IEEE,* vol. 77, no. 2, pp. 257–286, Feb. 1989.
[9] S. ten Brink, G. Kramer, and A. Ashikhmin, "Design of low-density parity-check codes for modulation and detection," *IEEE Trans. Commun.,* vol. 52, no. 4, pp. 670–677, Apr. 2004.
[10] D. Divsalar, S. Dolinar, C. R. Jones, and K. Andrews, "Capacity-approaching protograph codes," *IEEE J. Sel. Areas Commun.,* vol. 27, no. 6, pp. 876–888, Sept. 2001.